Annals of Physics 412 (2020) 168020

Contents lists available at ScienceDirect

Annals of Physics

journal homepage: www.elsevier.com/locate/aop

Interpretation of the anomaly in the diffuseness parameter of the Woods–Saxon potential for light fusion reactions using the effects of nuclear matter equation of state

R. Gharaei *, M.R. Yazdi

Department of Physics, Sciences Faculty, Hakim Sabzevari University, P.O. Box 397, Sabzevar, Iran

ARTICLE INFO

Article history:
Received 9 July 2019
Accepted 29 October 2019
Available online 11 November 2019

Keywords:
Light fusion reactions
Surface diffuseness parameter
Cold NM incompressibility

ABSTRACT

The present study has been aimed at understanding the role of nuclear matter (NM) incompressibility effects on the description of the problem of the abnormally large diffuseness parameter of the Woods–Saxon (WS) potential for the fusion reactions induced by the light-mass nuclei. In order to assess this aim, we simulate theoretically the saturation properties of NM within the framework of the double-folding (DF) model for a total of 26 colliding systems with condition $64 \leq Z_1Z_2 \leq 204$ for charge product of their participant nuclei. It is shown that the DF model supplemented with the effects of nuclear matter equation of state (EOS) provides an appropriate description for measured fusion cross sections of our selected systems at around and above barrier energies. We find that the diffuseness parameters of the equivalent WS potential fitted to the DF model in the fusion barrier region are ranging from 0.62 to 0.71 fm, whereas this range is increased to $a_{WS} = 0.66 - 0.81$ fm after modeling the incompressibility effects. Our results show that the extracted values of the diffuseness parameter based on the modified form of the DF model follow an increasing trend with the charge product Z_1Z_2. We also present for the first time a discussion on a decreasing linear dependence of the diffuseness parameter of the nucleus–nucleus potential on the nuclear incompressibility constant K.

* Corresponding author.
E-mail address: r.gharaei@hsu.ac.ir (R. Gharaei).

https://doi.org/10.1016/j.aop.2019.168020
0003-4916/

1. Introduction

Interaction potential between two nuclei is an essential factor for the interpretation of nuclear fusion reactions and determination of their cross sections. This potential generally consists of three parts; short-range nuclear attraction, centrifugal term and large-range Coulomb repulsion. It is well recognized that two latter parts can be calculated with high accuracy whereas some aspects of nuclear interactions are still not understood. However, during recent decades various theoretical models have been developed to estimate the strength of the nuclear interactions in fusion reactions. These models involve phenomenological ion–ion potential such as the Bass model [1,2] and proximity potential [3], or fully microscopic many-body approaches such as the time-dependent Hartree–Fock (TDHF) [4] which incorporates all of the dynamical entrance channel effects. These effects include the neck formation, particle exchange, internal excitations, collective surface vibrations, giant resonances and deformation effects, see for example Refs. [5–9]. Note that the fully microscopic TDHF theory also enables us to analyze the energy-dependence of the ion–ion potential for heavy-ion fusion reactions [10,11].

One of the standard models for real nuclear potential is the energy-independent Woods–Saxon (WS) form which is defined as follows,

$$V_{\mathrm{N}}^{\mathrm{WS}}(r) = \frac{-V_0}{1+\exp(\frac{r-R_{\mathrm{WS}}}{a_{\mathrm{WS}}})}. \tag{1}$$

In this relation, r refers to the separation distance between the centers of mass of the target and projectile. It is obvious that this form of potential can be defined by three parameters: the nuclear potential depth V_0, the average radius $R_{\mathrm{WS}} = r_0(A_1^{1/3} + A_2^{1/3})$ and the surface diffuseness parameter a_{WS}. One of the most challenging problems in the context of theoretical studies of heavy-ion fusion reactions is the inconsistency of the obtained values of the diffuseness parameter to fit simultaneously the experimental data of the elastic scattering cross sections and fusion cross sections. Generally, this parameter defines the potential slope in the tail region of the Coulomb barrier. One should keep in mind that the diffuseness parameters were extracted from a least-squares fit to the elastic scattering data that are around 0.63 fm [12–14]. Contrary to what would be expected for elastic scattering, it is shown that the required values for reproducing the experimental data of fusion cross sections approximately are ranging from $a_{\mathrm{WS}} = 0.75$ to 1.5 fm [15–21]. For example, the authors analyzed systematically the experimental data of fusion excitation functions of 47 fusion reactions at above Coulomb barrier energies using WS potential to extract the values of diffuseness parameter [17]. They performed the calculations of the real nuclear potentials with a fixed value of 100 MeV for potential depth parameter V_0. This value is relatively close to the potential depths of the standard forms of the WS parametrization of nuclear potential such as the Akyüz–Winther model [22]. The obtained results reveal that the empirical diffuseness parameters determined by fitting precise fusion cross sections are significantly greater than the expected values deduced from the elastic scattering data. The findings may reflect the necessity of a new dynamical approach for the calculations related to the complete fusion channel of two approaching nuclei.

The reason for the large discrepancies in the diffuseness parameters extracted from scattering and fusion analysis has not yet been fully understood. However, during recent years various attempts have been done to explain the anomaly in the diffuseness parameter of the nucleus–nucleus potential in heavy-ion fusion reactions [17,23–25]. One possible reason is that the elastic scattering is sensitive mainly to the surface region of the nuclear interaction potential whereas the fusion reactions are sensitive to both surface and inner regions of this potential. In reality, it is now understandable that the true shape of nuclear potential for heavy-ion fusion reactions departs from the standard form of WS potential at shorter distances. Another possible explanation of the large apparent diffuseness might result from the effect of energy dependence of the interaction potential and result in the dynamical characters of the fusion reaction which are related to the dynamical evolutions of the density distributions during the collision process [24–26].

In recent years, great attention has been paid to the effects of accounting for the nuclear matter (NM) equation of state (EOS) on the calculations of the nuclear potential and fusion excitation functions for medium- and heavy-mass fusion systems, see for example [23,27–32]. These effects

enable us to study theoretically the role of the nuclear incompressibility in the nucleon–nucleon (NN) interactions. A literature survey shows that simulating the NM incompressibility effects in the medium- and heavy-mass systems not only causes the appearance of a shallow pocket in the inner regions of the ion–ion potential but it also affects the shape of nuclear potential in the regions near the Coulomb barrier radius [23,28,29]. Under these conditions, it can be expected that the tail region of the nucleus–nucleus potential becomes sensitive to account for modeling the repulsive core effects in the NN interactions. So, it would be interesting to see whether the properties of cold nuclear matter may can be regarded as an appropriate physical reason for justifying the diffuseness anomaly in complete-fusion channel of two reacting nuclei. In the present paper, we focus on the fusion reactions induced by light-mass nuclei because the theoretical studies regarding the analysis of the effect of nuclear matter EOS on this mass region are very limited. In fact, our study is the first systematically attempt to achieve a suitable answer to the mentioned question using the study of 26 light colliding systems with the reaction charge product $64 \leq Z_1Z_2 \leq 204$. To simulate the NM incompressibility effects, we have adopted the double-folding (DF) potential model supplemented by an additional repulsive core potential which is due to the presence of the Pauli exclusion principle in the NN interactions [27,33,34]. It is remarkable that, within the framework of this microscopic approach, the nuclear potential can be obtained by integrating a NN interaction over the matter distributions of target and projectile [35]. Moreover, the strength of the repulsive interaction, as it was already discussed in the literature by [27,28], is proportional to the overlapping volume of the reacting nuclei. However, for light fusion reactions this volume is smaller compared to intermediate and heavy-mass systems. In this situation, we are motivated to analyze primarily the importance of the repulsive core effects in reproducing the energy-dependent behavior of the experimental fusion cross sections of our selected reactions. Finally, it should be noted that the equivalent diffuseness parameter $a_{\rm WS}$ in each of the presently studied reactions is determined by fitting the modified DF potential with a WS form in the region of the fusion barrier radius. The most important finding of the present study is to access a decreasing systematic behavior for the extracted values of the diffuseness parameter $a_{\rm WS}$ as a function of the nuclear matter incompressibility constant K.

This paper is organized as follows. Section 2 gives the relevant details of the theoretical framework used to simulate the saturation properties of cold nuclear matter in the NN interactions. Section 3 is devoted to the analysis of the influence of repulsive core potential on the calculations of the interaction potentials and fusion cross sections. In this section, a discussion is also presented about the dependence of the diffuseness parameter of WS potential on the nuclear matter incompressibility constant K. The conclusions drawn from the present analysis are given in Section 4.

2. Theoretical frameworks for simulating the incompressibility effects

As earlier stated, based on the proposed approach in Refs. [27,28] one can simulate the effects of NM incompressibility in the nucleon–nucleon interactions within the framework of the DF potential model. One common physical assumption used in this microscopic potential is the use of the frozen density or the sudden approximation. In this case, the approaching speed of two reacting nuclei is fast and comparable with their nucleons speed. In fact, it can be assumed that the density distributions of the nuclei are taken to be unchanged (or frozen) during the fusion process. The DF model is commonly used to calculate the real part of optical potential in the elastic and inelastic scattering [35–37]. However, in recent studies of the heavy-ion fusion reactions it has been employed to evaluate the strength of the nuclear interactions between two colliding nuclei, for example, see Refs. [38–40]. According to the DF model, one can obtain the nuclear potential by folding the densities of projectile and target with the density-dependent M3Y effective interactions of the Paris-CDM3Y6 type [41] as follows,

$$V_{\rm DF}(\mathbf{R}) = \int d\mathbf{r}_1 \int d\mathbf{r}_2 \rho_1(\mathbf{r}_1)\rho_2(\mathbf{r}_2)\upsilon_{NN}(\mathbf{r}_{12} = \mathbf{R} + \mathbf{r}_2 - \mathbf{r}_1). \tag{2}$$

Here, we have used two-parameter Fermi–Dirac (2PF) distribution function supplemented by the Hartree–Fock–Bogoliubov (HFB) calculations [42] for parametrization of the density distributions of

the reacting nuclei,

$$\rho_{2\mathrm{PF}}(r) = \frac{\rho_0}{1 + \exp\left[(r - R_0)/a_0\right]}, \tag{3}$$

The radius R_0 and diffuseness a_0 parameters of the proton and neutron density distributions we used are listed in Table 1. The results of the previous literature for heavy-ion fusion reactions show that the DF model predicts an unphysical form for the nuclear potential at short internuclear distances [28,29,43,44]. To cure this deficiency, it is suggested that the model should also contain a short-ranged repulsion potential which can be calculated via the DF integral, Eq. (2), with a zero-range interaction as $\upsilon_{\mathrm{rep}}(\mathbf{r}_{12}) = V_{\mathrm{rep}}\delta(\mathbf{r}_{12})$ for its central part as follows,

$$V_{\mathrm{rep}}(\mathbf{R})\,|_{R=0} = \int d\mathbf{r}_1 \int d\mathbf{r}_2 \rho_1(\mathbf{r}_1) V_{\mathrm{rep}}\delta(\mathbf{r}_{12})\rho_2(\mathbf{r}_2). \tag{4}$$

It is visible from the above relation that the calculations of the repulsive core potential must be performed for complete overlapping configuration of two reacting nuclei. Besides, it is here assumed that the diffuseness parameter of the density distributions of target and projectile is equal to a_{rep} [28]. With this assumption, we will deal with two adjustable parameters V_{rep} and a_{rep} to estimate the repulsive core term. For each of the considered reactions, the repulsive parameters should be selected in a manner that the modified form of the DF potential provides the best fit to the experimental data of the fusion barrier height. Moreover, the calculated value of the nuclear potential at $R = 0$ be in agreement with the predicted value obtained from the following condition [27],

$$V_N(0) \approx \frac{A_p}{9} K. \tag{5}$$

This equation relates the total nuclear potential at the complete overlapping region of density distributions to the nuclear incompressibility constant K as well as to the mass number of the projectile nucleus A_p. To obtain the strength of the incompressibility of cold NM, we consider the following definition,

$$K = 9\left(\rho^2 \frac{\partial^2 \varepsilon}{\partial \rho^2}\right)_{\rho=\rho_0}, \tag{6}$$

where $\rho_0 = 0.161\ \mathrm{fm}^{-3}$ is the saturation density of NM. It is visible that the definition of this constant is related to the curvature of the energy per particle of nuclear matter $\varepsilon(\rho, \delta)$, where $\delta = (\rho_n - \rho_p)/\rho$ is the relative neutron excess of the compound (fused) nucleus. It can be estimated from the EOS predicted by the Thomas–Fermi model [45],

$$\varepsilon(\rho, \delta) = \varepsilon_F\left[A(\delta)\left(\frac{\rho}{\rho_0}\right)^{2/3} + B(\delta)\left(\frac{\rho}{\rho_0}\right) + C(\delta)\left(\frac{\rho}{\rho_0}\right)^{5/3}\right], \tag{7}$$

herein ε_F is the Fermi energy of normal NM.

3. Calculations and results

We select 26 complete fusion reactions induced by light-mass nuclei covering the range of $64 \leq Z_1Z_2 \leq 204$ for charge product of their reacting nuclei as well as the range of $10.92 \leq Q\ (\mathrm{MeV}) \leq 19.96$ for their Q-values. The reaction with the smallest Z_1Z_2 considered here is $^{16}\mathrm{O}+^{16}\mathrm{O}$, whereas the largest one is $^{37}\mathrm{Cl}+^{26}\mathrm{Mg}$. Note, all nuclei are assumed to be spherical in nature. In addition, the present survey includes all kinds of colliding systems involving symmetric ($N = Z$) and asymmetric ($N \neq Z$) nuclei. Using a simple calculation, one can find out that the sum of radii $R_1 + R_2$ of the participant nuclei in the presently studied reactions lies between 6.04 and 7.55 fm. This range reflects the discrepancy between the size of the present systems with those analyzed in earlier works, such as the fusion of $^{12}\mathrm{C}+^{92}\mathrm{Zr}$ [23] with $R_1 + R_2 = 8.16$ fm.

Table 1
The radius and diffuseness parameters of the proton and neutron density distributions, Eq. (3), based on the HFB method [42].

Nucleus	R_{0n} (fm)	a_{0n} (fm)	R_{0p} (fm)	a_{0p} (fm)
^{16}O	2.6519	0.4602	2.6986	0.4469
^{17}O	2.7494	0.4566	2.7054	0.4543
^{18}O	2.8135	0.4729	2.7335	0.4658
^{19}F	2.8348	0.4673	2.8143	0.4551
^{24}Mg	3.0409	0.4570	3.0794	0.4505
^{25}Mg	3.0839	0.4635	3.0920	0.4575
^{26}Mg	3.1067	0.4832	3.1118	0.4593
^{27}Al	3.1361	0.4782	3.1595	0.4646
^{28}Si	3.1671	0.4726	3.1984	0.4750
^{30}Si	2.8772	0.6053	3.2510	0.4737
^{32}S	3.0846	0.5460	3.1540	0.5144
^{34}S	3.2279	0.5144	3.3659	0.5177
^{35}Cl	3.2637	0.5144	3.4175	0.5268
^{37}Cl	3.5786	0.4919	3.5321	0.4919

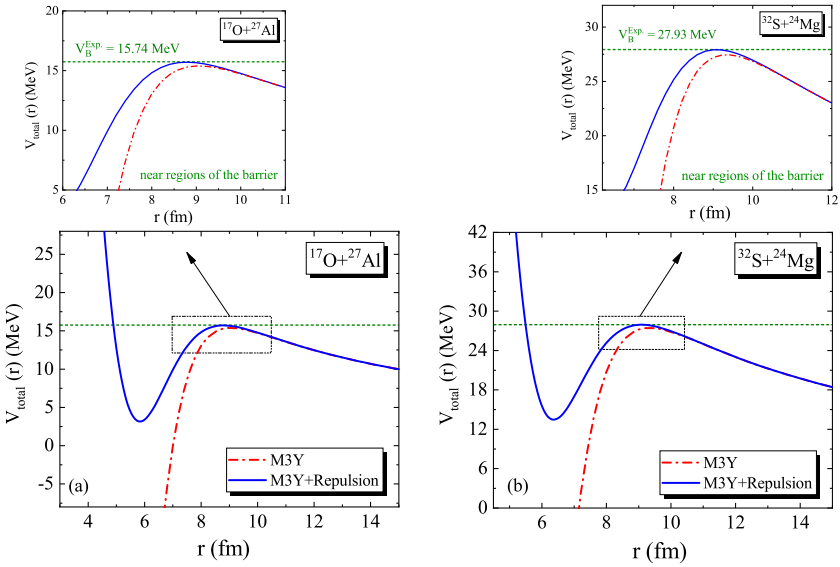

Fig. 1. Entrance channel potentials for (a) ^{17}O+^{27}Al, and (b) ^{32}S+^{24}Mg obtained from the M3Y-DF (red dash-dotted line) and M3Y+Repulsion (blue solid line) potential models. In each panel, the experimental barrier heights are also indicated by green short-dashed line.

3.1. Evaluating the double folding potentials

To understand the importance of the saturation properties of cold NM on the complete fusion channel of light nuclei, in the first step, we need to calculate the interaction potentials using the microscopic M3Y-DF model. In the next step, we follow the procedure proposed in the previous section to simulate theoretically the saturation properties of NM in the nucleon–nucleon interactions of the presently studied fusion reactions. We plot in Fig. 1 the Coulomb plus nuclear potential based on the M3Y-DF potential with and without considering the corrective effects of the cold NM for two arbitrary colliding systems ^{17}O+^{27}Al and^{32}S+^{24}Mg. It is remarkable that the results of the modified form of the DF model are marked as "M3Y+Repulsion". The figure also includes the experimental values of the barrier height (the horizontal short-dashed lines) for comparison.

Table 2
The calculated values of the parameters used in calculating the repulsive core potential for different colliding systems and the associated nuclear incompressibility K and pocket energy V_{pocket}.

Reaction	Z_1Z_2	a_{rep} (fm)	V_{rep} (MeV fm^3)	K (MeV)	V_{pocket} (MeV)
^{16}O+^{16}O	64	0.405	596.2	234.44	−0.64
^{17}O+^{16}O	64	0.387	578.1	234.08	−5.04
^{18}O+^{16}O	64	0.441	649.8	233.09	4.64
^{16}O+^{27}Al	104	0.427	541.7	234.23	1.47
^{17}O+^{27}Al	104	0.437	553.1	233.63	3.16
^{18}O+^{27}Al	104	0.449	564.1	232.71	4.22
^{16}O+^{28}Si	112	0.426	536.6	234.44	2.08
^{19}F+^{27}Al	117	0.414	532.4	233.7	−1.94
^{24}Mg+^{30}Si	168	0.487	566.7	233.9	15.35
^{28}Si+^{24}Mg	168	0.416	581.5	234.44	11.76
^{28}Si+^{26}Mg	168	0.466	613	233.9	20.64
^{30}Si+^{24}Mg	168	0.468	599.9	233.9	14.79
^{30}Si+^{26}Mg	168	0.497	609.5	232.45	18.43
^{32}S+^{24}Mg	192	0.441	579.6	234.44	13.48
^{32}S+^{25}Mg	192	0.43	558	234.32	7.16
^{32}S+^{26}Mg	192	0.435	552.1	233.98	5.4
^{34}S+^{24}Mg	192	0.399	561.8	233.98	3.09
^{28}Si+^{28}Si	196	0.459	592.4	234.44	22.9
^{28}Si+^{30}Si	196	0.503	588	233.98	22.74
^{30}Si+^{30}Si	196	0.496	544	232.71	6.43
^{35}Cl+^{24}Mg	204	0.443	612.5	234.33	19.23
^{35}Cl+^{25}Mg	204	0.465	624.6	234.01	23.25
^{35}Cl+^{26}Mg	204	0.484	632.5	233.5	25.78
^{37}Cl+^{24}Mg	204	0.411	620.9	233.5	15.6
^{37}Cl+^{25}Mg	204	0.449	646.3	232.82	23.69
^{37}Cl+^{26}Mg	204	0.473	657.5	231.99	27.04

On the basis of the results presented in Fig. 1, one can find out that the corrective effects of the cold NM incompressibility mainly affect the shape of interaction potential at the inner regions of the Coulomb barrier. It would mean that we are confronted with the appearance of a shallow pocket in the entrance channel potential which is produced by the M3Y+Repulsion double folding potential. In addition, it is seen in this figure that the modified form of the potential attains a thicker and higher fusion barrier than the original version of the M3Y double folding model. In fact, for the fusion of ^{17}O+^{27}Al and ^{32}S+^{24}Mg, we find that the agreement with the data, when using the M3Y+Repulsion potential, is much better than the one provided by the M3Y-DF potential. In this situation, it is important to remind the DF potential without repulsion predicts correctly the ion–ion potential only for the peripheral collisions where the density distributions are gently overlapping and thus the frozen density assumption is less questionable.

The repulsive parameters a_{rep} and V_{rep} we obtain for all 26 colliding systems are presented in Table 2. In this table we have also listed the values of the incompressibility constant K of the compound nuclei predicted by the Thomas–Fermi model, Eq. (6), together with the obtained values of the pocket energy V_{pocket} that appears in the inner regions of the Coulomb plus nuclear potential. Depending on Table 2, one can find out that the extracted values of the strength of the repulsive core potential are ranging from $V_{\text{rep}} = 532.4$ to 657.5 MeV. This may reflect the fact that the strength of the repulsive interaction can be sensitive to the variations in the mass and atomic numbers of the reacting nuclei. In what follows we intend to explore the validity of this physical result for our selected mass range. For this purpose, the variations trend of the obtained values of V_{rep} is shown in Fig. 2 as a function of $Z_1Z_2/(A_1^{1/3}+A_2^{1/3})$ ratio. From an inspection of this figure, one can find out that the strength of repulsive interaction for different projectile–target combinations increases linearly by enhancing the values of the mentioned ratio. One can parameterize the linear trend using the

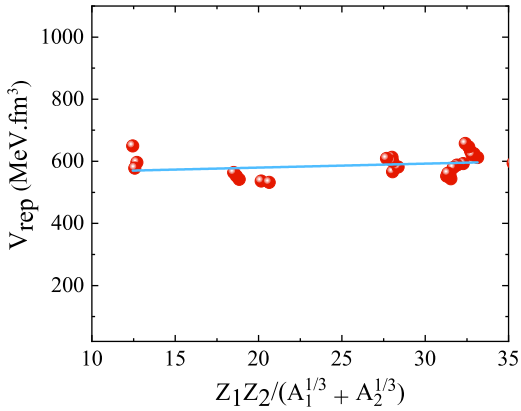

Fig. 2. The variations trend of the calculated values of the strength of the repulsive core potential $V_{\rm rep}$ as a function of the $Z_1Z_2/(A_1^{1/3}+A_2^{1/3})$ ratio for our selected mass range.

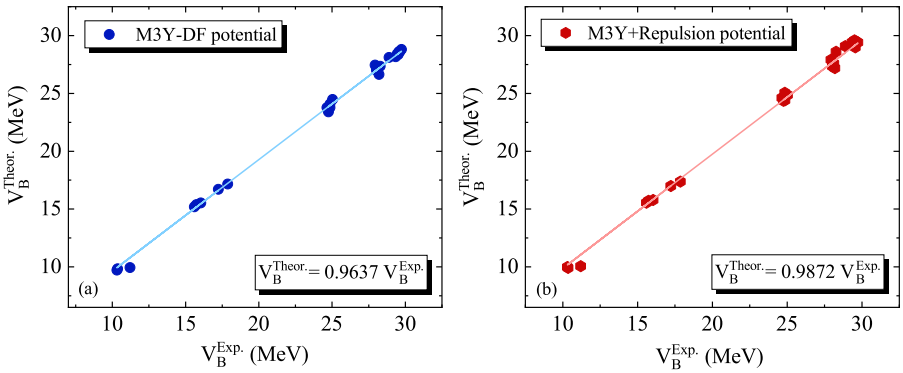

Fig. 3. The variations trend of the theoretical fusion barrier heights $V_B^{\rm Theor.}$ (in MeV) as a function of the experimental fusion barrier heights $V_B^{\rm Exp.}$ (in MeV). Parts (a), and (b) show the results with M3Y-DF and M3Y-Repulsion potential models, respectively.

following relation,

$$V_{\rm rep} = 1.275\left(\frac{Z_1Z_2}{A_1^{1/3}+A_2^{1/3}}\right) + 554.21, \tag{8}$$

where A_i and Z_i are the mass and atomic numbers of the reacting nuclei, respectively. The above formula gives a direct method to calculate the strength of the repulsive interaction in our selected mass range when the numerical values of (A, Z) quantities are specified for the colliding system. Another point to note in Table 2 is that the estimated values of the constant K vary within the $K \simeq 232$–235 MeV range. This range implies that the average value of the nuclear incompressibility for our considered fusion reactions is consistent with the value commonly indicated in various studies, namely $K \simeq 234$ MeV [31,46,47].

The precise values of the calculated barrier heights based on the M3Y-DF and M3Y+Repulsion potential models for all 26 studied reactions are presented in Table 3. To test the validity of the present work, in Fig. 3, we have compared our outcome with the corresponding experimental data available in the literature. This figure, in fact, shows the theoretical values of the barrier height $V_B^{\rm Theor.}$ as a function of the experimental values $V_B^{\rm Exp.}$ for our selected mass range. One can observe

Table 3
Comparison of the barrier heights between the results of DF potential model and experimental data for the presently studied fusion systems. The first and second columns denote the different reaction systems and experimental data. The third and forth columns indicate the barrier height of the original and modified forms of the DF potential models, respectively.

Reaction	$V_B^{\text{Exp.}}$ (MeV)	V_B^{M3Y} (MeV)	$V_B^{\text{M3Y+Repulsion}}$ (MeV)
^{16}O+^{16}O	11.20	9.94	10.06
^{17}O+^{16}O	10.36	9.84	9.92
^{18}O+^{16}O	10.31	9.72	9.98
^{16}O+^{27}Al	16.04	15.53	15.78
^{17}O+^{27}Al	15.74	15.39	15.71
^{18}O+^{27}Al	15.60	15.19	15.55
^{16}O+^{28}Si	17.23	16.71	16.99
^{19}F+^{27}Al	17.87	17.17	17.38
^{24}Mg+^{30}Si	24.65	23.78	24.62
^{28}Si+^{24}Mg	25.03	24.48	24.86
^{28}Si+^{26}Mg	24.85	24.08	25.06
^{30}Si+^{24}Mg	24.86	23.78	24.41
^{30}Si+^{26}Mg	24.75	23.41	24.37
^{32}S+^{24}Mg	27.93	27.45	27.91
^{32}S+^{25}Mg	28.13	27.25	27.58
^{32}S+^{26}Mg	28.03	27.01	27.33
^{34}S+^{24}Mg	28.06	27.18	27.38
^{28}Si+^{28}Si	28.89	28.12	29.09
^{28}Si+^{30}Si	28.28	27.35	28.60
^{30}Si+^{30}Si	28.74	26.65	27.19
^{35}Cl+^{24}Mg	29.73	28.81	29.41
^{35}Cl+^{25}Mg	29.62	28.60	29.49
^{35}Cl+^{26}Mg	29.51	28.37	29.58
^{37}Cl+^{24}Mg	29.56	28.62	28.99
^{37}Cl+^{25}Mg	29.45	28.42	29.24
^{37}Cl+^{26}Mg	29.34	28.17	29.43

that the DF model supplemented with a short-ranged repulsion potential generates the barrier heights which are in more agreement with the experimental data than those obtained by its original version.

3.2. Evaluating the fusion cross sections

Here and in the following we are interested in knowing the influence of the modeling of the saturation effects of cold NM on the fusion excitation functions for our selected mass range. From the theoretical point of view, the simplest way to address the calculations of heavy-ion fusion cross sections is to use the single-barrier penetration model (SBPM) [48] wherein the projectile and target are assumed to be structureless charge particle. On the one side, the SBPM usually gives reasonable agreement with the measured fusion cross sections at above barrier energies [48–50]. On the other hand, the experimental incident energies for the presently studied reactions are ranged around near and above Coulomb barrier energies. As a typical example of this reality, Fig. 4 shows that the minimum incident energy required for the occurrence of the ^{32}S+^{24}Mg fusion reaction, $E_{\text{c.m.}} = 26.04$ MeV, is comparable with the Coulomb barrier height, $V_B = 27.91$ MeV, deduced from the M3Y+Repulsion potential model. Under these conditions, it is reasonable to use here the SBPM for calculating the theoretical values of the fusion cross sections.

Calculations were performed for all 26 systems. The obtained results reveal that the experimental data is substantially overestimated by using the M3Y-DF model. While the fusion cross sections are suppressed by imposing the NM incompressibility effects on the nuclear potential. In fact, the calculations based on the M3Y+Repulsion model are in good agreement with the experimental data.

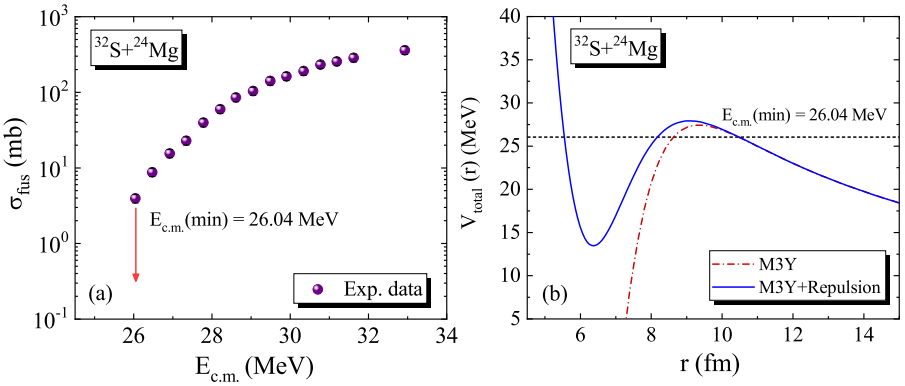

Fig. 4. Search for the validity of SBPM for calculating the theoretical values of the fusion cross sections for an arbitrary colliding system $^{32}S+^{24}Mg$. The left and right panels describe the energy-dependent behavior of the experimental data of the fusion cross sections and the radial behavior of total interaction potential based on the M3Y and M3Y+Repulsion potentials, respectively. The minimum incident energy $E_{c.m.} = 26.04$ MeV is comparable with the Coulomb barrier height obtained from the M3Y+Repulsion potential.

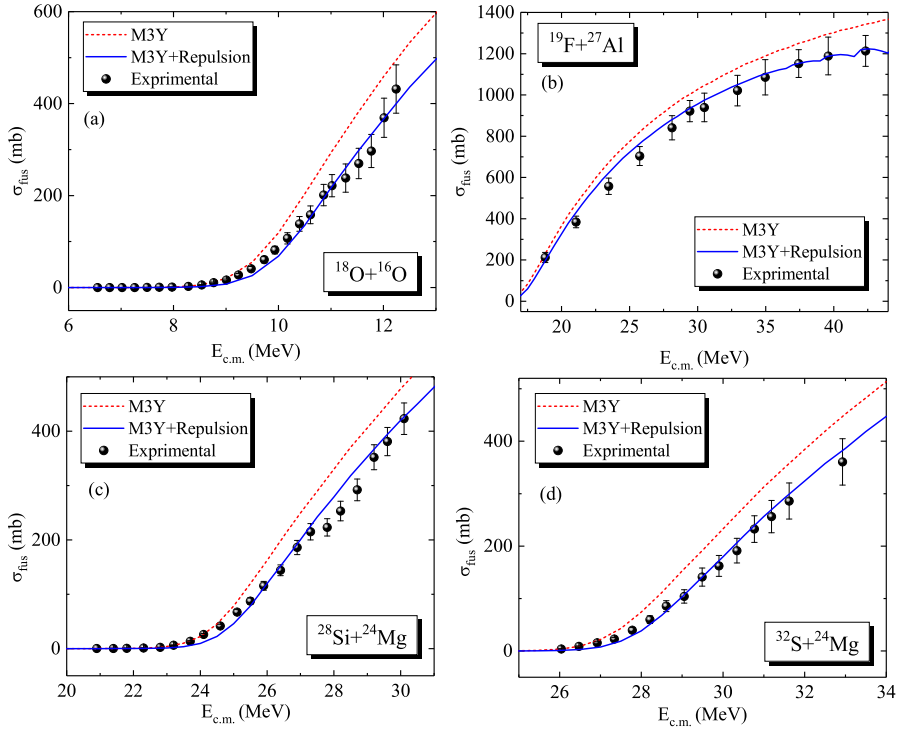

Fig. 5. Experimental fusion excitation functions for the colliding systems (a) $^{18}O+^{16}O$, (b) $^{19}F+^{27}Al$, (c) $^{28}Si+^{24}Mg$ and (d) $^{32}S+^{24}Mg$ compared with the calculations performed by the M3Y and M3Y+Repulsion potential models.

This situation is illustrated by Fig. 5, which includes the results of $^{18}O+^{16}O$, $^{19}F+^{27}Al$,$^{28}Si+^{24}Mg$ and $^{32}S+^{24}Mg$ colliding systems, and by Fig. 6, which includes the results of $^{16}O+^{16}O$,$^{18}O+^{27}Al$,

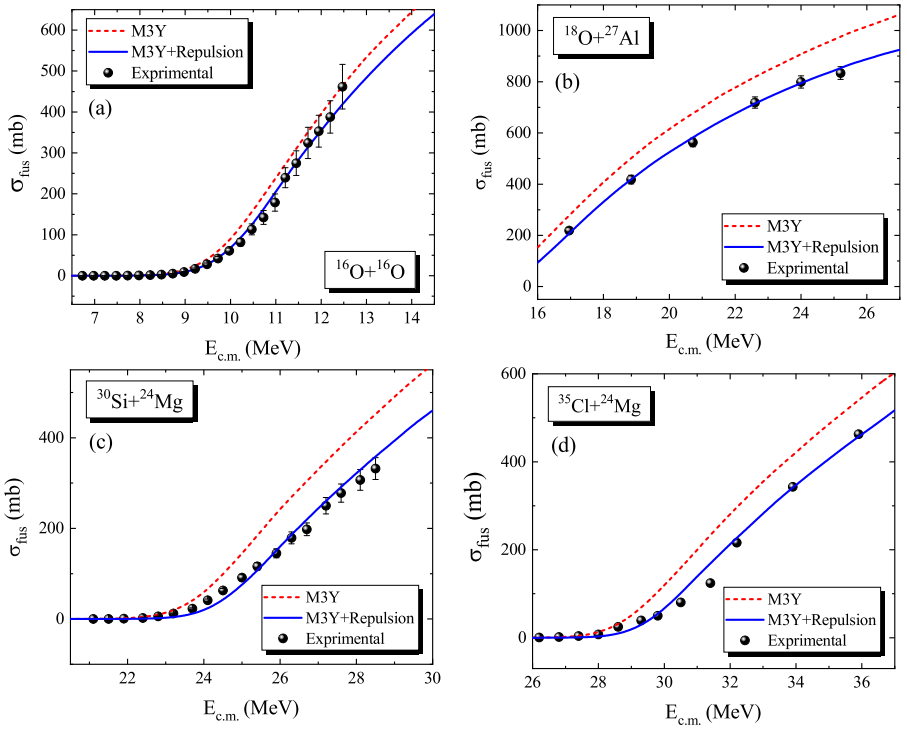

Fig. 6. Same as Fig. 5 but for the colliding systems (a) ^{16}O+^{16}O, (b) ^{18}O+^{27}Al, (c) ^{30}Si+^{24}Mg and (d) ^{35}Cl+^{24}Mg.

^{30}Si+^{24}Mg and ^{35}Cl+^{24}Mg colliding systems, for instance. Here the measured and calculated fusion cross sections are presented as a function of the center-of-mass energy $E_{\text{c.m.}}$.

3.3. Effect of nuclear EOS on the potential diffuseness

To analyze the corrective effects of cold NM on the surface diffuseness of the nuclear potential, we extract the values of the equivalent diffuseness by a least-square fitting the M3Y and M3Y+Repulsion potentials with a WS form in the region of the fusion barrier radii. The extracted values for this parameter are listed in Table 4. To gain further insight, we have analyzed the energy-dependent behavior of the experimental fusion cross sections for each of the considered reactions using the real bare WS nuclear potential. The values of the parameter $a_{\text{WS}}^{\text{Exp.}}$ derived from fitting the experimental data are presented in the last column of Table 4. One can consider these values as a precise scale of the diffuseness parameter for our selected reactions. In addition, it must be noted that the fitting processes have been performed with a fixed potential depth of $V_0 = 100$ MeV [17,24]. On the basis of the tabulated results, we find that the obtained diffuseness parameters from the modified form of the DF potential (ranging from 0.66 to 0.81 fm) are greater than those obtained by its original form (ranging from 0.62 to 0.71 fm). One can thus conclude that the repulsive core effects in nucleonic interactions providing a reason for a larger value of the parameter a_{WS} for heavy-ion fusion reactions. In order to achieve further understanding, we have calculated the percentage difference between the theoretical and experimental values of the diffuseness parameter using the following relation,

$$\Delta a_{\text{WS}}(\%) = \frac{a_{\text{WS}}^{\text{Theor.}} - a_{\text{WS}}^{\text{Exp.}}}{a_{\text{WS}}^{\text{Exp.}}} \times 100. \tag{9}$$

Table 4
The extracted values of the diffuseness parameter of the WS potential based on the M3Y and M3Y+Repulsion models for our selected fusion systems. In the last column, we have presented the values of the parameter a_{WS} deduced from fitting the corresponding experimental data of the fusion cross section. The systems are listed with respect to their increasing Z_1Z_2 values.

Reaction	Z_1Z_2	a_{WS}^{M3Y}	$a_{WS}^{M3Y+Repulsion}$	$a_{WS}^{Exp.}$
$^{16}O+^{16}O$	64	0.62	0.68	0.72
$^{17}O+^{16}O$	64	0.62	0.66	0.74
$^{18}O+^{16}O$	64	0.63	0.73	0.73
$^{16}O+^{27}Al$	104	0.62	0.68	0.74
$^{17}O+^{27}Al$	104	0.62	0.69	0.75
$^{18}O+^{27}Al$	104	0.63	0.72	0.76
$^{16}O+^{28}Si$	112	0.63	0.69	0.74
$^{19}F+^{27}Al$	117	0.63	0.67	0.76
$^{24}Mg+^{30}Si$	168	0.67	0.76	0.80
$^{28}Si+^{24}Mg$	168	0.63	0.69	0.79
$^{28}Si+^{26}Mg$	168	0.64	0.77	0.77
$^{30}Si+^{24}Mg$	168	0.67	0.75	0.82
$^{30}Si+^{26}Mg$	168	0.67	0.80	0.80
$^{32}S+^{24}Mg$	192	0.66	0.73	0.83
$^{32}S+^{25}Mg$	192	0.65	0.69	0.86
$^{32}S+^{26}Mg$	192	0.65	0.69	0.84
$^{34}S+^{24}Mg$	192	0.65	0.67	0.86
$^{28}Si+^{28}Si$	196	0.63	0.76	0.79
$^{28}Si+^{30}Si$	196	0.68	0.79	0.81
$^{30}Si+^{30}Si$	196	0.71	0.76	0.81
$^{35}Cl+^{24}Mg$	204	0.66	0.71	0.84
$^{35}Cl+^{25}Mg$	204	0.65	0.75	0.83
$^{35}Cl+^{26}Mg$	204	0.65	0.79	0.81
$^{37}Cl+^{24}Mg$	204	0.62	0.69	0.82
$^{37}Cl+^{25}Mg$	204	0.64	0.75	0.83
$^{37}Cl+^{26}Mg$	204	0.63	0.81	0.82

The calculated values of $\Delta a_{WS}(\%)$ based on the theoretical models M3Y and M3Y+Repulsion are shown in Fig. 7, plotted against the charge product $Z_1Z_2/(A_1^{1/3} + A_2^{1/3})$ of our selected fusion reactions. It is obvious from the figure that the imposing of the NM incompressibility effects on the calculations of the interaction potential improves the agreement between the theoretical and experimental values of the parameter a_{WS}.

The increasing trend of the diffuseness parameter of the WS potential with increase of Z_1Z_2 has been previously shown for range $Z_1Z_2 \geq 224$ [17,23]. Herein, we are interested in investigating such trend for our selected mass range with charge product $Z_1Z_2 \leq 204$. So, in Fig. 8, we show the behavior of the extracted values of the parameter a_{WS} as a function of Z_1Z_2 based on the M3Y+Repulsion potentials. It is obvious that the diffuseness parameters have an increasing trend with the increase of Z_1Z_2 values. The red-upward triangles and blue-downward triangles in Fig. 8 show the results which are respectively taken from the previous works [17,23]. There exists acceptable consistency between the results of our selected mass range and those extracted for heavier systems.

It is worth while to examine the behavior of the diffuseness parameters versus the incompressibility of the compound (fused) nuclei corresponding to the M3Y+Repulsion potentials. Such behavior is shown in Fig. 9. In this figure, we have also displayed the values of the diffuseness parameter of WS potential deduced from the interacting systems of ^{12}C, ^{16}O, ^{28}Si and ^{35}Cl on ^{92}Zr [23]. Note, the authors of that study investigated the importance of the NM equation of state on the interaction potential and also fusion cross sections of four medium-heavy mass fusion systems, including the collision of^{12}C, ^{16}O, ^{28}Si and ^{35}Cl projectiles with the same target ^{92}Zr. For these reactions, the values of charge product Z_1Z_2 lying between 240 and 680 are clearly larger than those obtained for the presently studied reactions. Moreover, one is confronted with the smaller range of the nuclear incompressibility constant, namely $K = 229$ to 231 MeV, in these

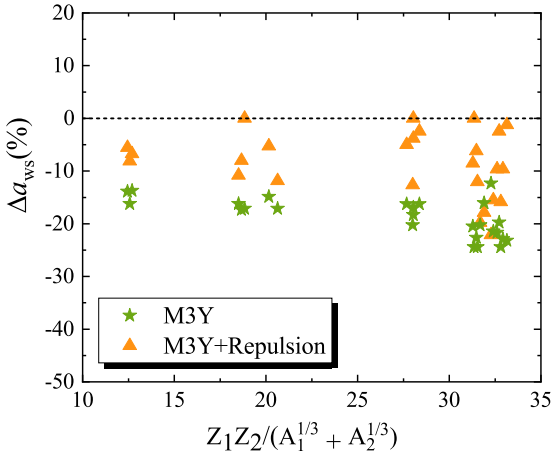

Fig. 7. The percentage difference between the theoretical and experimental values of the diffuseness parameter of WS potential as a function of the $Z_1Z_2/(A_1^{1/3}+A_2^{1/3})$ ratio based on the original and modified forms of the DF model for our selected mass range. For details, see the text.

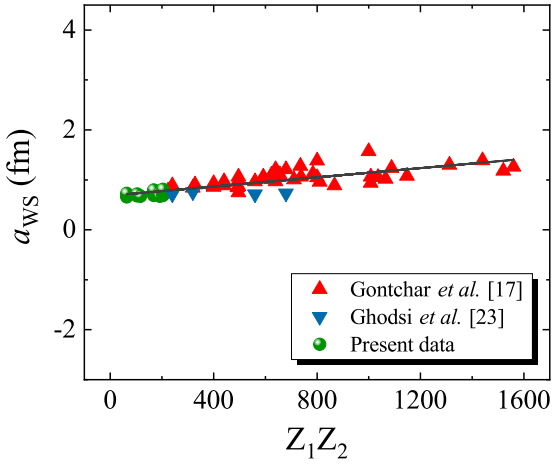

Fig. 8. The behavior of the extracted values of the parameter a_{WS} based on the present M3Y+Repulsion potentials (green solid circle) as a function of the charge product Z_1Z_2 of the reacting nuclei. The results of the previous works are also presented: Gontchar et al. [17] (red-upward triangles) and Ghodsi et al. [23] (blue-downward triangles). (For interpretation of the references to color in this figure legend, the reader is referred to the web version of this article.)

four fusion systems. The inspection of the figure reveals that the obtained diffuseness parameters from the M3Y+Repulsion potential are systematically larger than 0.63 fm. In addition, we note the diffuseness parameters follow a linear decreasing trend with increase of the strength of incompressibility of cold nuclear matter in the whole range $229 < \mathrm{K\,(in\ MeV)} < 235$. The equation of the fitted line to these values is given by,

$$a_{WS}(K) = -0.0073K + 2.4406. \tag{10}$$

This equation gives a direct method to determine the diffuseness parameter of WS potential when the value of the constant K is specified for the reacting systems.

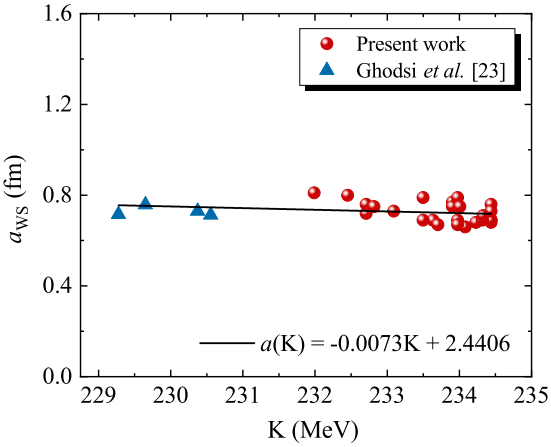

Fig. 9. The extracted diffuseness parameters by considering the saturation property of cold nuclear matter as a function of the incompressibility constant K for all considered fusion systems. The blue-upward triangles show the results of the $^{12}C+^{92}Zr$, $^{16}O+^{92}Zr$, $^{28}Si+^{92}Zr$ and $^{35}Cl+^{92}Zr$ colliding systems which have been studied in Ref. [23].

4. Summary and conclusions

To summarize, we have performed a systematic study of the nuclear fusion reactions in the mass region of light nuclei to describe the large values of the diffuseness parameter in the fusion process on the basis of the saturation property of cold NM. The microscopic DF model is used to simulate theoretically this property in the nucleon–nucleon interactions of 26 fusion reactions with condition $64 \leq Z_1Z_2 \leq 204$. In the DF model, the NN interaction is selected as CDM3Y6-Paris type. The calculations of the fusion cross sections have been performed by the SBPM because the experimental measurements of fusion cross sections for our selected reactions are available at near- and above-barrier energies. The main results of the present study can be summarized as follows.

- The obtained results confirm that the interaction potential is mainly sensitive to the modeling of the nuclear incompressibility effects at the shorter distances. However, it is shown that these effects can increase the agreement between the theoretical and experimental values of the Coulomb barrier height for fusion reactions induced by the light colliding nuclei.
- The saturation effects of cold NM can be responsible for the description of the fusion cross sections of light colliding systems at energies near and above the Coulomb barrier.
- We have succeeded to present a systematic behavior for the strength of the repulsive core potential by fitting the calculated values of the parameter V_{rep} versus the $Z_1Z_2/(A_1^{1/3}+A_2^{1/3})$ quantity. The obtained results indicate that the numerical values of V_{rep} have an increasing trend with an increase in $Z_1Z_2/(A_1^{1/3}+A_2^{1/3})$ ratio going from $^{16}O+^{16}O$ to $^{37}Cl+^{26}Mg$. Though that further systematic investigations are needed in order to achieve a deep understanding of such correlation.
- The imposing of the corrective effects of the nuclear matter incompressibility on the nucleus–nucleus potential leads to an increase in the values of the diffuseness parameters of the WS potential.
- We have proposed a K-dependent parametrization formula for determining the values of the diffuseness parameter represented in the WS potential in heavy-ion fusion reactions. It is shown that the parameter a_{WS} has a decreasing trend with the strength of the incompressibility constant K. This implies that the surface diffuseness of nuclear potential can reduce by increasing the levels of the stiffness of nuclear matter.

Declaration of competing interest

The authors declare that they have no known competing financial interests or personal relationships that could have appeared to influence the work reported in this paper.

References

[1] R. Bass, Nuclear Phys. A 231 (1974) 45.
[2] R. Bass, Nuclear Reactions with Heavy Ions, Springer Verlag, New York, 1980.
[3] J. Blocki, J. Randrup, W.J. Swiatecki, C.F. Tsang, Ann. Phys., NY 105 (1977) 427.
[4] A.S. Umar, V.E. Oberacker, Phys. Rev. C 74 (2006) 021601, (R).
[5] J.W. Negele, Rev. Modern Phys. 54 (1982) 913.
[6] C. Simenel, Eur. Phys. J. A 48 (2012) 152.
[7] A.S. Umar, V.E. Oberacker, Phys. Rev. C 71 (2005) 034314.
[8] C.I. Pardi, P.D. Stevenson, K. Xu, Phys. Rev. E 89 (2014) 033312.
[9] P.-G. Reinhard, Lu Guo, J. Maruhn, Eur. Phys. J. A 32 (2007) 19.
[10] K. Washiyama, D. Lacroix, Phys. Rev. C 78 (2008) 024610.
[11] A.S. Umar, C. Simenel, V.E. Oberacker, Phys. Rev. C 89 (2014) 034611.
[12] P.R. Christensen, A. Winther, Phys. Lett. B 65 (1976) 19.
[13] L.C. Chamon, L.C. Chamon, D. Pereira, E.S. Rossi Jr., C.P. Silva, H. Dias, L. Losano, C.A.P. Ceneviva, Nuclear Phys. A 597 (1996) 253.
[14] C.P. Silva, M.A.G. Alvarez, L.C. Chamon, et al., Nuclear Phys. A 679 (2001) 287.
[15] J.O. Newton, C.R. Morton, M. Dasgupta, J.R. Leigh, J.C. Mein, D.J. Hinde, H. Timmers, K. Hagino, Phys. Rev. C 64 (2001) 064608.
[16] I.I. Gontchar, D.J. Hinde, M. Dasgupta, J.O. Newton, Nuclear Phys. A 722 (2003) C479.
[17] J.O. Newton, R.D. Butt, M. Dasgupta, D.J. Hinde, I.I. Gontchar, C.R. Morton, K. Hagino, Phys. Rev. C 70 (2004) 024605.
[18] A. Mukherjee, D.J. Hinde, M. Dasgupta, K. Hagino, J.O. Newton, R.D. Butt, Phys. Rev. C 75 (2007) 044608.
[19] K. Hagino, T. Takehi, A.B. Balantekin, N. Takigawa, Phys. Rev. C 71 (2005) 044612.
[20] J.O. Newton, R.D. Butt, M. Dasgupta, D.J. Hinde, I.I. Gontchar, C.R. Morton, K. Hagino, Phys. Lett. B 586 (2004) 219.
[21] K. Hagino, N. Rowley, M. Dasgupta, Phys. Rev. C 67 (2003) 054603.
[22] Ö. Akyüz, A. Winther, in: R.A. Broglia, C.H. Dasso, R. Richi (Eds.), Proceedings of the International School of Physics, Enrico Fermi, Course LXXVII, Varenna, 1979, North-Holland, Amsterdam, 1981.
[23] O.N. Ghodsi, V. Zanganeh, Nuclear Phys. A 846 (2010) 40.
[24] M. Singh, S.S. Duhan, R. Kharab, Modern Phys. Lett. A 26 (2011) 2129.
[25] V. Zanganeh, R. Gharaei, N. Wang, Phys. Rev. C 95 (2017) 034620.
[26] K. Hagino, M. Dasgupta, I.I. Gonchar, D.J. Hinde, C.R. Morton, J.O. Newton, Proceedings of the Fourth ItalyJapan Symposium on Heavy-Ion Physics, Tokyo, Japan, World Scientific, Singapore, 2002, pp. 87–98, nucl-th/0110065.
[27] S. Misicu, H. Esbensen, Phys. Rev. Lett. 96 (2006) 112701.
[28] S. Misicu, H. Esbensen, Phys. Rev. C 75 (2007) 034606.
[29] R. Gharaei, J. Phys. G: Nucl. Part. Phys. 44 (2017) 045108.
[30] C.L. Jiang, et al., Phys. Rev. Lett. 113 (2014) 022701.
[31] C.L. Jiang, et al., Phys. Rev. C 82 (2010) 041601, (R).
[32] H. Esbensen, C.L. Jiang, A.M. Stefanini, Phys. Rev. C 82 (2010) 054621.
[33] T. Fliessbach, Z. Phys. 247 (1971) 117.
[34] C. Simenel, A.S. Umar, K. Godbey, M. Dasgupta, D.J. Hinde, Phys. Rev. C 91 (2017) 031601, (R).
[35] G.R. Satchler, W.G. Love, Phys. Rep. 183 (1979) 55.
[36] C.W. Glover, R.I. Cutler, K.W. Kemper, Nucl. Phys. A 341 (1980) 137.
[37] M.E. Brandan, G.R. Satchler, Phys. Rep. 285 (1997) 143.
[38] I.I. Gontchar, D.J. Hinde, M. Dasgupta, J.O. Newton, Phys. Rev. C 69 (2004) 024610.
[39] M. Rashdan, J. Phys. G: Nucl. Part. Phys. 22 (1996) 139.
[40] W.M. Seif, J. Phys. G: Nucl. Part. Phys. 30 (2004) 1231.
[41] G. Bertsch, J. Borysowicz, H. McManus, W.G. Love, Nuclear Phys. A 284 (1977) 399.
[42] [http://www-nds.iaea.org/RIPL-2/masses.html].
[43] O.N. Ghodsi, R. Gharaei, Phys. Rev. C 85 (2012) 064620.
[44] O.N. Ghodsi, R. Gharaei, Phys. Rev. C 84 (2011) 024612.
[45] W.D. Myers, W.J. Swiatecki, Phys. Rev. C 57 (1998) 3020.
[46] C.L. Jiang, B.B. Back, H. Esbensen, J.P. Greene, R.V.F. Janssens, D.J. Henderson, H.Y. Lee, C.J. Lister, M. Notani, R.C. Pardo, N. Patel, K.E. Rehm, D. Seweryniak, B. Shumard, X. Wang, S. Zhu, S. Mi sicu, P. Collon, X.D. Tang, Phys. Rev. C 78 (2008) 017601.
[47] H. Esbensen, X. Tang, C.L. Jiang, Phys. Rev. C 84 (2011) 064613.
[48] A.B. Balantekin, N. Takigawa, Rev. Modern Phys. 70 (1998) 77.
[49] K. Hagino, N. Takigawa, Progr. Theoret. Phys. 128 (2012) 1061.
[50] M. Dasgupta, N. Rowley, A.M. Stefanini, Annu. Rev. Nucl. Part. Sci. 48 (1998) 401.